

Hansan Liu · Jie Li · Zhongru Zhang
Zhengliang Gong · Yong Yang

The effects of sintering temperature and time on the structure and electrochemical performance of $\text{LiNi}_{0.8}\text{Co}_{0.2}\text{O}_2$ cathode materials derived from sol-gel method

Received: 25 September 2002 / Accepted: 22 October 2002 / Published online: 26 March 2003
© Springer-Verlag 2003

Abstract $\text{LiNi}_{0.8}\text{Co}_{0.2}\text{O}_2$ cathode materials were synthesized by the sol-gel method using citric acid as a chelating agent. The effects of sintering temperature and time on the structure and electrochemical performance of the materials were investigated. The materials were characterized by X-ray diffraction, together with refinement analysis by the Rietveld method. The results showed that sintering temperature and time had significant influence on the structure of the materials. The lattice parameters (a , c , c/a and volume) and the amount of Ni in the Li 3a site showed a peak shape change with sintering temperature and time. The sample sintering at 998 K for 24 h showed the best ordering layered structure with the maximum c/a ratio and the least amount of Ni on the Li 3a site. The charge-discharge experiments also indicated that the sample had the best electrochemical properties, with an initial capacity of 181 mA h/g and a capacity retention of 82.9% after 50 cycles at a 0.1 C rate between 3.0 V and 4.2 V. In addition, the compositional homogeneity of these cathode materials derived using the sol-gel method was demonstrated by scanning electron microscopy/energy dispersive analysis.

Keywords Lithium nickel cobalt oxide · Sol-gel method · Rietveld refinement · Lithium ion batteries

Introduction

Recently, lithium nickel cobalt oxides, $\text{LiNi}_{1-x}\text{Co}_x\text{O}_2$, have been investigated intensively as alternative cathode materials for LiCoO_2 in lithium ion batteries [1, 2, 3, 4].

The layered structure of LiCoO_2 , which is the dominant cathode material of current commercial lithium ion batteries, has some limitations due to its high cost, moderate capacity and toxicity. Hence, new cathode materials are needed to replace the LiCoO_2 material. The analogous structure LiNiO_2 was initially thought of as a potential alternative material because of its higher specific capacity and lower cost. However, it was found that LiNiO_2 has several drawbacks, such as difficult synthesis of stoichiometric products, poor cyclability and unsatisfactory thermal stability [5, 6, 7]. For attaining improved cathode materials, $\text{LiNi}_{1-x}\text{Co}_x\text{O}_2$ solid solutions are proposed as strong potential candidates to replace LiCoO_2 [8]. These solid solutions show improved properties with better cyclability and thermal stability [9, 10].

$\text{LiNi}_{1-x}\text{Co}_x\text{O}_2$ solid solutions are traditionally synthesized by solid-state methods at elevated temperatures (1073–1173 K) over a prolonged period of time (~48 h) [11]. This high-temperature synthesis leads to problems of poor stoichiometry control, non-homogeneity and large particle size. It also entails a significant expense invested in the production process. These problems have prompted many researchers to design and develop new “soft chemistry” synthesis routes such as the sol-gel method [12, 13] and the co-precipitation method [14, 15]. Julien et al. [16, 17] recently reported the synthesis of $\text{LiNi}_{0.5}\text{Co}_{0.5}\text{O}_2$ and $\text{LiNi}_{0.6}\text{Co}_{0.4}\text{O}_2$ by sol-gel methods using various chelating agents. Kweona et al. [18] also synthesized $\text{Li}_x\text{Ni}_{0.85}\text{Co}_{0.15}\text{O}_2$ using the poly(vinyl alcohol) (PVA) precursor method. All of these nominal low-temperature methods include a sintering process for the sol-gel precursor. In the sintering process, the reaction temperature and time must be high and long enough to favor ion diffusion, but lithium loss, associated with a partial reduction of Ni^{3+} , can occur spontaneously. Thus, the change of the material’s structure and electrochemical performance with the sintering temperature and time is to be expected. Alcantara et al. [19] investigated the effect of temperature and composition on the $\text{LiNi}_{1-x}\text{Co}_x\text{O}_2$ materials synthesized by solid-state

H. Liu · J. Li · Z. Zhang · Z. Gong · Y. Yang (✉)
State Key Laboratory for Physical Chemistry of Solid Surfaces
and Department of Chemistry, Xiamen University,
361005 Xiamen, P.R. China
E-mail: yyang@xmu.edu.cn
Tel.: +86-592-2185753
Fax: +86-592-2185753

methods and concluded that the sintering temperature could not be below 1023 K in that case. Gover et al. [20] also reported that the appropriate sintering conditions for $\text{LiNi}_{0.8}\text{Co}_{0.2}\text{O}_2$ derived by co-precipitation was 998 K and 48 h. In this paper, we synthesized $\text{LiNi}_{0.8}\text{Co}_{0.2}\text{O}_2$ samples at various temperatures (923–1750 K) and times (12–36 h) by the sol-gel method using citric acid as a chelating agent. The effect of sintering temperature and time on the structure and electrochemical properties of the $\text{LiNi}_{0.8}\text{Co}_{0.2}\text{O}_2$ materials was investigated.

Experimental

Preparation of cathode materials

$\text{LiNi}_{0.8}\text{Co}_{0.2}\text{O}_2$ powders were synthesized by the sol-gel method using citric acid as the chelating agent. The synthesis procedure includes three steps: the sol-gel process, a pre-calcination process and the calcination process. In the sol-gel process, nitrate salts of Li, Ni and Co, in stoichiometric amounts, were dissolved in distilled water and mixed well with citric acid (the acid-to-metal ions ratio was 1:1), also dissolved in distilled water, to form a transparent dark-green solution. The mixture was stirred at 353 K for 5 h to form a sol, and then a gel under constant heating and stirring to evaporate water for about 12 h. The gel was heated at 393 K for 24 h to form a dry gel, which was put into a Mullf oven for pre-calcination at 773 K for 6 h. Lastly, the dark-brownish decomposed powder was heated in a horizontal quartz tube oven and calcined at various temperatures (923–1073 K) and various times (12–36 h) with a fixed oxygen flux ($500 \text{ cm}^3/\text{min}$). The temperature-controlling programs for the pre-calcination and calcination processes were established according to a TGA-DTG curve. The thermal analysis was carried out on a Netzsch STA 400 analyzer with 100 mL/min of flowing air and a heating rate of $20 \text{ }^\circ\text{C}/\text{min}$ in the temperature range 323–1273 K.

Structural and compositional characterization

The $\text{LiNi}_{0.8}\text{Co}_{0.2}\text{O}_2$ samples were characterized by powder X-ray diffraction (XRD), using a Rigaku Rotaflex D/max-C diffractometer with a graphite monochromator and $\text{Cu K}\alpha$ radiation operated at 40 kV and 30 mA. Data were collected in the range $10\text{--}90^\circ$ using a step size of 0.02° and a counting time of 2 s per step. Rietveld refinement structural analyses were carried out using the software General Structure Analysis System (GSAS) [21]. The morphology and compositional homogeneity of the samples were assessed using a scanning electron microscopy (LEO 1530 field emission SEM, Oxford Instruments) operated at 15 kV and fitted with an energy dispersive analysis (EDA) detector (INCA energy and crystal system, ISIS 300).

Electrochemical measurements

The capacity and cyclability of the synthesized samples were assessed using CR2025 coin cells. The cathode was prepared by mixing 85% of the active material with 10% carbon black and 5% poly(vinylidene fluoride) (PVDF). The mixture was made into a slurry by ball milling using NMP as the solvent. The electrodes were formed by coating the slurry onto Al foils and pressing at 16 MPa after drying overnight at 393 K in a vacuum. The cells were assembled with the cathode as prepared, with lithium metal as the anode, and with Celgard 2300 film as a separator. The electrolytes were 1 M LiPF_6 dissolved in EC+DMC (1:1 volume ratio). Cell assembly was carried out in an argon-filled glove box

(Master 100 Lab, Braun, Germany), where water and oxygen concentrations were kept less than 4 ppm. Charge-discharge testing was performed galvanostatically at a 0.1 C rate between 3.0 V and 4.2 V by an Arbin BT-2043 battery test system.

Results and discussion

Thermal analysis

Figure 1 shows TGA-DTG curves of the dry-gel precursor prepared for the pre-calcination and calcination processes. There are four distinct regions of weight loss on the TGA curve in the temperature range 323–1273 K. According to previous studies [16, 22], the weight loss of the precursor ($\sim 11.7\%$) below 473 K could be due to desorption of superficial and structural water. In the temperature range 473–610 K there is a large weight loss ($\sim 34.2\%$) due to the decomposition of nitrate and/or the dehydration of metal citrate to aconitate [23]. Then a sharp drop of weight ($\sim 17.4\%$) appears between 610 K and 673 K, which was attributed to the combustion of aconitate and its complex. After that, a weight loss ($\sim 10.0\%$) occurs in the temperature range 673–773 K, corresponding to the decomposition of the residual organic components. In addition, a minor weight loss (3.0%) appears between 973 K and 1073 K after a constant period from 773 K to 973 K, corresponding to the reaction of Li_2CO_3 and $\text{Ni}_{10.8}\text{Co}_{0.2}\text{O}$ to form $\text{LiNi}_{0.8}\text{Co}_{0.2}\text{O}_2$, and a constant weight loss occurs continuously above 1073 K corresponding to O_2 evaporation from $\text{LiNi}_{0.8}\text{Co}_{0.2}\text{O}_2$, similar to the reaction mechanism of LiNiO_2 derived using the sol-gel technique [24]. According to the results, the corresponding temperature-control programs for the pre-calcination process for thorough decomposition of the organic and nitrate components was established, and the temperature range of 973–1073 K for studies of the effects of sintering temperature on the calcination process was selected. After optimization of the sintering temperature,

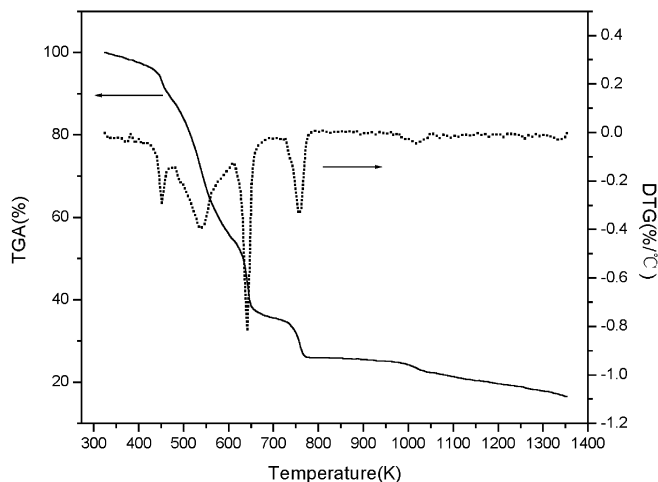


Fig. 1 TGA-DTG curves of the dry-gel precursor, operated in air and with a scan rate of $20 \text{ }^\circ\text{C}/\text{min}$

the time range of 12–36 h was selected for investigating the effect of sintering time at the fixed sintering temperature of 998 K.

SEM-EDAX analysis

According to the SEM micrographs, the surface of the sample particles was covered by many microcrystallites with a rectangular shape, and the average size of the microcrystallites was about 0.1–2.0 μm , which changed with sintering temperature and time. The size of the microcrystallites increased from ca. 0.3 μm for the samples synthesized at 973 K for 24 h to ca. 2.0 μm for the samples synthesized at 1073 K for 24 h, and from ca. 0.1 μm for the samples synthesized at 998 K for 12 h to ca. 1.0 μm for the samples synthesized at 998 K for 30 h.

Like lithium nickel cobalt oxide materials derived using the solid-state method, the compositional homogeneity on a microscopic scale is one of the most difficult features to achieve. Delmas et al. [7] has reported that $\text{LiNi}_{0.7}\text{Co}_{0.15}\text{Al}_{0.15}\text{O}_2$ obtained by direct synthesis from the oxides is not homogeneous at the long-range scale seen by XRD, and the $\text{LiNi}_{1-x}\text{Co}_x\text{O}_2$ system shows domains of cobalt aggregation on an atomic scale as detected by NMR. The sol-gel method is thought to allow a better mixing of the reactants at the atomic level and produces higher homogeneous materials. SEM-EDAX analyses of $\text{LiNi}_{0.8}\text{Co}_{0.2}\text{O}_2$ samples as prepared were used to confirm this opinion. We selected several spots at different zones and several areas (about 0.001 mm^2) from the sample synthesized at 998 K for 24 h for EDAX analyses. Owing to the non-sensitivity of lithium to the elemental microprobe, quantitative analysis of the composition could not be obtained, but the relative heights of the nickel and cobalt peaks gave a good indication of the relative amounts of the two elements in the sample. The results showed that the transition metal elemental distribution at various points is almost uniform and the average ratio of Ni/Co (0.7950:0.2050) is roughly the same as the nominal composition (0.8:0.2) of the sample, which confirms the homogeneity of $\text{LiNi}_{0.8}\text{Co}_{0.2}\text{O}_2$ materials derived using the sol-gel technique.

XRD characterization and Rietveld refinement

The $\text{LiNi}_{0.8}\text{Co}_{0.2}\text{O}_2$ samples sintered at various temperatures and times were characterized by XRD. All of the patterns can be indexed to a single phase of the $\alpha\text{-NaFeO}_2$ type with the space group $R\bar{3}m$. As reported [25, 26], the ordering of the structure can be deduced from the XRD spectra with the intensity ratio $I_{(003)}/I_{(104)}$ and the degree of either (108)/(110) or (006)/(102) peak splitting. The $I_{(003)}/I_{(104)}$ peak ratios of the materials synthesized at various conditions are listed in Table 1. For the samples of the temperature series, the ratio of $I_{(003)}/I_{(104)}$ increases firstly from 1.43 at 973 K to 1.51 at

Table 1 The $I_{(003)}/I_{(104)}$ peak ratios of XRD patterns for the materials synthesized under various conditions

Temperature series (K) for 24 h time	Peak ratios	Time series (h) at 998 K temperature	Peak ratios
973	1.43	12	1.25
998	1.51	18	1.23
1023	1.34	24	1.51
1048	1.29	30	1.31
1073	1.23	36	1.27

998 K and then decreases from 1.34 at 1023 K to 1.26 at 1073 K. Similar changes also occur in the samples of the time series. The peak ratio value increases from the sample of 12 h to that of 24 h and then decreases to that of 36 h. The sample sintered at 998 K for 24 h shows the highest $I_{(003)}/I_{(104)}$ ratio. Meanwhile, the samples show various degrees of (108)/(110) and (006)/(102) peak splitting. It appears that both sintering temperature and time have a significant influence on the structure of the samples. In addition, we also synthesized the sample sintered at 923 K for 24 h, for which the XRD pattern shows a set of small exceptional peaks that can be indexed to Li_2CO_3 . The sample will not be discussed in the following sections, but it indicates that the sintering temperature should exceed at least 923 K for a sample with a pure phase, which is consistent with the result of the TGA-DTG analysis. In order to determine the structure more accurately, Rietveld refinement analyses of these XRD patterns were performed.

The Rietveld refinements were carried out assuming that all the samples have the layered $\alpha\text{-NaFeO}_2$ type structure with space group $R\bar{3}m$ and atomic positions as follows: 3a site at (0,0,0); 3b site at (0,0,0.5); and 6c site at (0,0,0.24). Since neutron diffraction experiments [4] have verified that Co only lies at the 3b site and Li is almost never at the 3b site, we adopt the model that only Ni goes to the 3a site and Ni and Co are considered as the same atom in the 3b site owing to the limit of X-rays to discern Ni and Co. The initial values of the lattice and thermal parameters were obtained from the data of a LiNiO_2 single crystal [27]. The refinement process followed strictly the Rietveld refinement guidelines formulated by the International Union of Crystallography Commission on Powder Diffraction [28]. The observed, calculated and difference plots for the sample sintered at 998 K for 24 h are shown in Fig. 2. The residual factors R_{wp} , R_{B} and goodness of fit χ^2 are listed in Table 2.

The changes of lattice parameters a , c , their ratio c/a and the lattice volume of samples derived from various temperatures and times are illustrated in Fig. 3. It is clear that a , c and V decrease from 973 K to 998 K, then increase from 998 K to 1073 K, as well as that the sample synthesized at 998 K has the minimum lattice parameters and volume. On the other hand, the ratio c/a has the reverse change tendency and the sample synthesized at 998 K has the maximum c/a ratio. It indicates that this sample has the best hexagonal ordering structure. The amounts of Ni in the 3a Li site (g_{Ni})

Fig. 2 Observed, calculated and difference XRD patterns for a $\text{LiNi}_{0.8}\text{Co}_{0.2}\text{O}_2$ sample sintered at 998 K for 24 h after Rietveld refinement

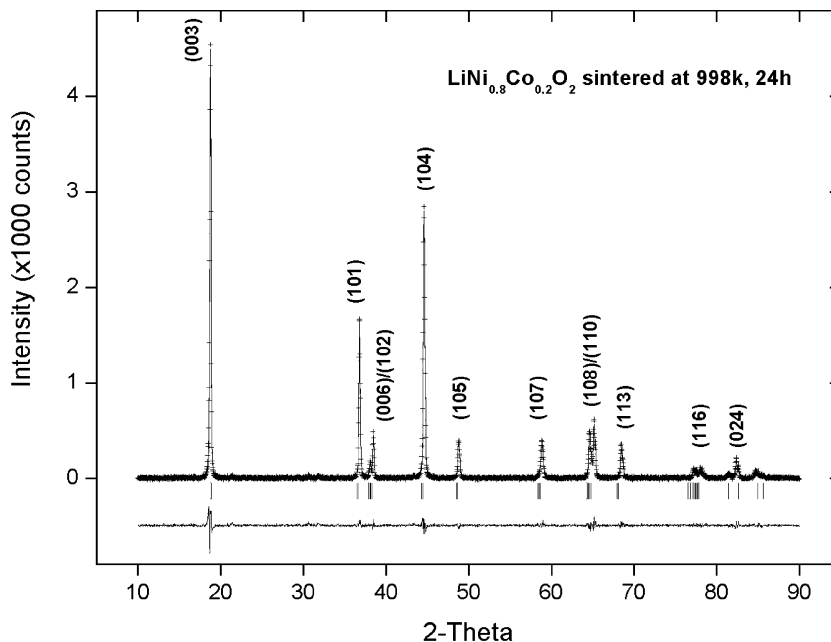


Table 2 Reliability factors for XRD Rietveld refinement

Synthesis conditions	R_{wp} (%) ^a	R_B (%) ^b	χ^2 ^c
12 h, 998 K	13.42	4.56	1.843
18 h, 998 K	13.04	3.20	1.830
24 h, 998 K	12.58	3.27	1.756
30 h, 998 K	13.00	3.15	1.720
36 h, 998 K	13.32	3.63	1.767
973K, 24 h	12.14	2.66	1.542
1023 K, 24 h	12.05	2.54	1.531
1048 K, 24 h	13.26	3.32	1.766
1073 K, 24 h	13.70	4.14	1.856

$$^a R_{wp} = [\sum_i |Y_i(\text{obs}) - Y_i(\text{calc})|^2 / \sum W_i Y_i^2(\text{obs})]^{1/2}$$

$$^b R_B = \sum_i |Y_i(\text{obs}) - Y_i(\text{calc})| / \sum Y_i(\text{obs})$$

$$^c \chi^2 = (R_{wp}/R_e)^2$$

shown in Fig. 4 also demonstrate this conclusion. The amount decreases firstly from 973 K to 998 K and then increases from 998 K to 1073 K, while the sample synthesized at 998 K has the minimum g_{Ni} (~ 0.011). The effect of sintering temperature implies that ion diffusion is the prevailing factor controlling the structure before 998 K and the Li content volatilization inverses to be the main factor after 998 K. At 998 K, a compromise of the two processes produces the sample with the best ordering layered structure.

Similar to the sintering temperature, the sintering time also has a significant influence on the structure of the samples. All of the parameters of the samples sintered for various times show peak-shape changes like the samples sintered at various temperatures. The sample sintered for 24 h shows the minimum a , c , V and g_{Ni} values and the maximum c/a ratio, which indicates the best ordering layered structure among the time series samples. The result shows that the crystallization is not complete if the time is shorter than 24 h and the Li

content volatilization becomes the key factor in controlling the structure if the time is longer than 24 h at a fixed sintering temperature of 998 K.

The bond angles and lengths from the refinement analyses are presented in Table 3, together with the thickness of slab (O-Ni-O) and inter-slab (O-Li-O) values. The changes of interatomic distances are closely relevant to the displacement of the atoms. Owing to $[\text{Ni}_z]_{3a}$ in the formula of $[\text{Li}_{1-z}\text{Ni}_z]_{3a}[\text{Ni}_{0.8}\text{Co}_{0.2}]_{3b}[\text{O}_2]_{6c}$, the Li-O, Ni-O and Ni-Ni bond lengths and slab and inter-slab thicknesses changed with the amount of Ni at the 3a site. Among all of the samples, the one sintered at 998 K for 24 h has the maximum Li-O length and inter-slab (O-Li-O) thickness and the minimum Ni-O and Ni-Ni lengths and slab (O-Ni-O) thickness, which matches the minimum amount of Ni in the 3a site. All of the results show that there is an optimum sintering condition for the $\text{LiNi}_{0.8}\text{Co}_{0.2}\text{O}_2$ material with the best ordering layered structure, which is 998 K and 24 h in this case. Compared with the direct solid-state method [19] and the co-precipitation method [20], the sol-gel technique can produce $\text{LiNi}_{0.8}\text{Co}_{0.2}\text{O}_2$ materials at lower sintering temperatures and shorter sintering times.

Electrochemical performance

The electrochemical properties of $\text{LiNi}_{0.8}\text{Co}_{0.2}\text{O}_2$ samples derived from the sol-gel technique sintered at various temperatures and times were tested galvanostatically at a 0.1 C rate between 3.0 V and 4.2 V. Table 4 presents the charge-discharge capacity and the loss of capacity of the first cycle for all the samples. As the sintering temperature and time increase, the charge capacity of the first cycle decreases gradually from 214 mA h/g at 973 K to 198 mA h/g at 1073 K and

Fig. 3 Change of lattice parameters a , c , V and c/a for $\text{LiNi}_{0.8}\text{Co}_{0.2}\text{O}_2$ samples synthesized at various sintering temperatures and times. The stars represent the time series and the circles represent the temperature series

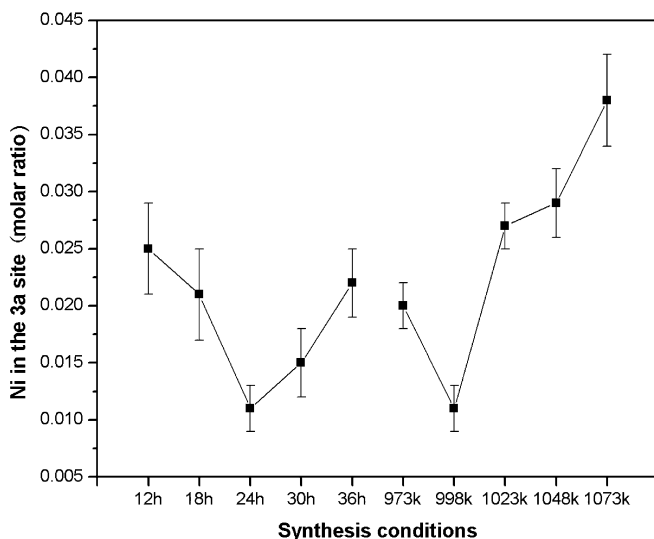
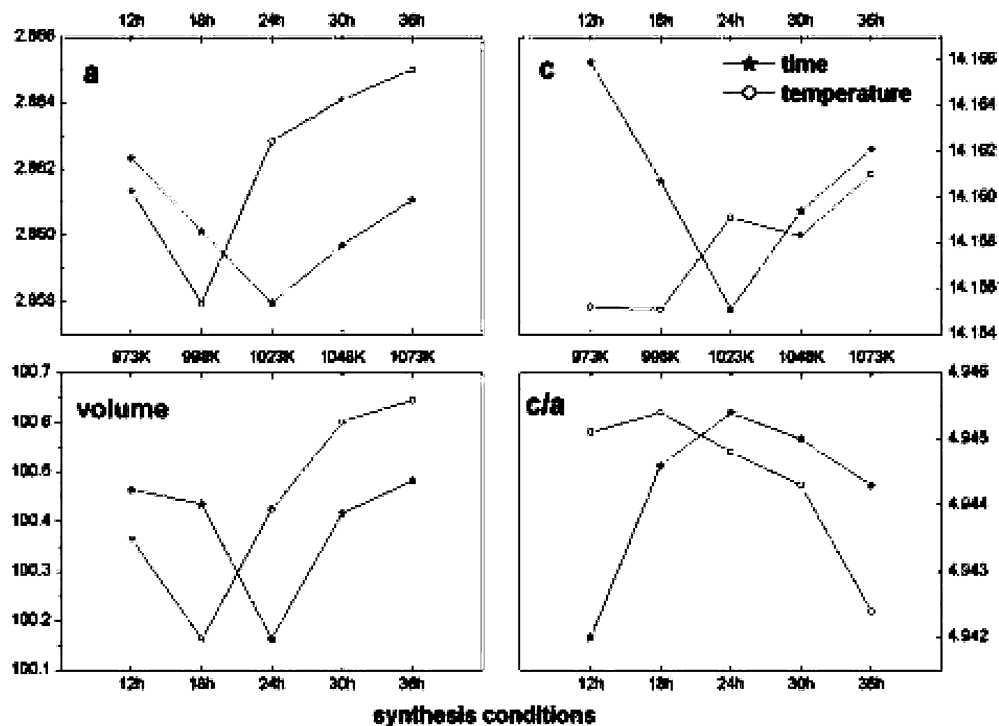


Fig. 4 The amount of Ni in the 3a Li site for $\text{LiNi}_{0.8}\text{Co}_{0.2}\text{O}_2$ samples synthesized at various sintering temperatures and times, calculated by Rietveld refinement

from 236 mA h/g at 12 h to 200 mA h/g at 36 h. It is thought that the degree of lithium volatilization increases with the increase of sintering temperature and time. After sintering at higher temperatures and for longer times, there are fewer lithium ions participating in the de-intercalation process of the first cycle as well as a lower charge capacity. However, no such effect was seen in the discharge capacity and loss of capacity for the first cycle. As shown in Table 4, the discharge capacity increases firstly and then decreases following the increasing of temperature and time, while the loss of capacity changes oppositely. It shows that the sample sintered at 998 K for 24 h has the best electrochemical properties among all of the samples. Figure 5 illustrates the charge-discharge curves and the cycling performance curve for this sample. The discharge capacities of this sample are 181 mA h/g and 183 mA h/g at the first and second cycles, respectively, with the capacity retention of 82.9% after 50 cycles.

There appears to be a correlation of the discharge capacity and the loss of capacity with the amount of Ni

Table 3 Bond angles and lengths and slab (NO_2) and inter-slab (LiO_2) thicknesses obtained from Rietveld refinement

Synthesis conditions	Li-O ₂ (Å)	Ni-O ₂ (Å)	Ni-Ni ₂ (Å)	O-Li-O ₂ (°)	O-Ni-O ₂ (°)	$S_{(\text{NiO}_2)}$ (Å) ^a	$I_{(\text{LiO}_2)}$ (Å) ^b
12 h, 998 K	2.0953(6)	1.9697(4)	2.8606(5)	86.10(5)	93.13(5)	2.5998	2.1185
18 h, 998 K	2.0975(6)	1.9657(4)	2.8623(5)	85.99(5)	93.26(5)	2.5838	2.1363
24 h, 998 K	2.1066(6)	1.9628(4)	2.8579(5)	85.79(5)	93.63(5)	2.5781	2.1471
30 h, 998 K	2.1032(6)	1.9632(4)	2.8609(5)	85.71(5)	93.61(5)	2.6034	2.1163
36 h, 998 K	2.1023(9)	1.9642(6)	2.8597(5)	85.71(9)	93.62(10)	2.6046	2.1173
973 K, 24 h	2.1014(6)	1.9630(4)	2.8613(6)	85.81(8)	93.57(9)	2.5970	2.1213
1023 K, 24 h	2.1042(7)	1.9636(5)	2.8628(4)	86.12(9)	93.33(9)	2.5789	2.1374
1048 K, 24 h	2.1027(9)	1.9653(6)	2.8641(4)	85.78(5)	93.66(10)	2.5975	2.1218
1073 K, 4 h	2.0959(8)	1.9680(6)	2.8650(4)	85.88(9)	93.59(10)	2.6037	2.1166

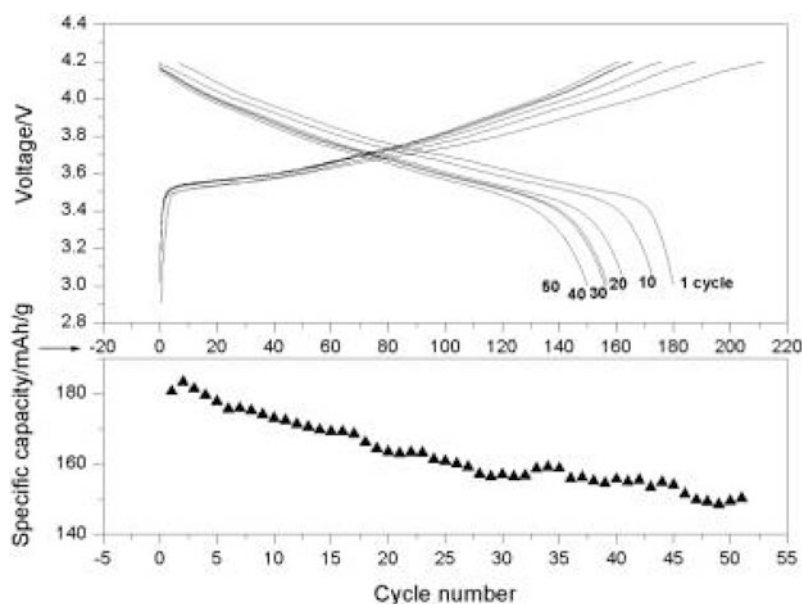
^a Slab thickness: $S_{(\text{NiO}_2)} = (2/3 - 2Z_{\text{O}})C_{\text{hex}}$

^b Interslab thickness: $I_{(\text{LiO}_2)} = C_{\text{hex}}/3 - S_{(\text{NiO}_2)}$

Table 4 Charge-discharge data of the first cycle for $\text{LiNi}_{0.8}\text{Co}_{0.2}\text{O}_2$ samples synthesized at various temperatures and times

Synthesis conditions	Charge (mA h/g)	Discharge (mA h/g)	Lost (mA h/g)	Efficiency (%)
12 h, 998 K	236.0	131.6	104.6	55.7
18 h, 998 K	221.1	162.8	48.6	73.6
24 h, 998 K	211.9	180.6	31.3	85.2
30 h, 998 K	208.1	174.3	33.8	83.8
36 h, 998 K	200.2	165.4	34.8	82.6
973 K, 24 h	214.3	170.6	39.7	79.6
1023 K, 24 h	198.9	166.0	32.9	83.5
1048 K, 24 h	190.2	152.9	37.3	80.4
1073 K, 24 h	197.6	157.3	40.3	79.6

Fig. 5 Charge-discharge curves and cycling performance curve of a $\text{LiNi}_{0.8}\text{Co}_{0.2}\text{O}_2$ sample synthesized at 998 K for 24 h



at the 3a Li site. Comparing Fig. 4 and Table 4, there is a similar tendency between the changes of discharge capacity and the efficiency of the first cycle and that of the amount of Ni in the 3a Li site. The highest discharge capacity (181 mA h/g) and the lowest loss of capacity (14.8%) at the first cycle correspond well to the minimum amount of Ni in the 3a Li site (~ 0.011) for the sample sintered at 998 K for 24 h. As reported [7], there would be a local collapse of the interlayer space during the de-intercalation process due to divalent nickel oxidation to trivalent nickel in the 3a Li site, and an irreversible capacity would be formed during the intercalation process due to the irreversibility of structural recovery. Thus, the effects of sintering temperature and time on the electrochemical properties depend on the changes of structure with the variety of sintering temperature and time.

Conclusions

$\text{LiNi}_{0.8}\text{Co}_{0.2}\text{O}_2$ materials were synthesized at various temperatures (923–1073 K) and times (12–36 h) by the sol-gel method using citric acid as a chelating agent. The

effects of sintering temperature and time on the structure and electrochemical properties were investigated. The results of XRD and Rietveld refinement showed that the lattice parameters and the amount of Ni in the 3a Li site had a peak value with the changes of temperature and time, and implied that there is an optimum sintering condition for the $\text{LiNi}_{0.8}\text{Co}_{0.2}\text{O}_2$ material with the best ordering layered structure, which is 998 K and 24 h in this case. The charge-discharge experiments also indicated that the sample had the maximum initial capacity (181 mA h/g) and the minimum capacity loss (14.8%) with a capacity retention of 82.9% after 50 cycles at a 0.1 C rate between 3.0 V and 4.2 V. The effects of sintering temperature and time on the structure matched well with the electrochemical properties. Compared with direct solid-state and co-precipitation methods, the sol-gel technique can produce $\text{LiNi}_{0.8}\text{Co}_{0.2}\text{O}_2$ materials at lower sintering temperatures and shorter sintering times. In addition, SEM-EDAX analysis verified the compositional homogeneity of the samples derived from the sol-gel method.

Acknowledgements This work was financially supported by the National Natural Science Foundation of China (nos. 29925310, 29833090).

References

1. Tarascon JM, Armand M (2001) *Nature* 414:361
2. Winter M, Besenhard JO, Spahr ME, Novak P (1998) *Adv Mater* 10:743
3. Alcantara R, Lavela P, Tirado JL, Zhecheva E, Stoyanova R (1999) *J Solid State Electrochem* 3:126
4. Lee KK, Kim KB (2000) *J Electrochem Soc* 147:1709
5. Broussely M, Biensan P, Simon B (1999) *Electrochim Acta* 45:9
6. Ohzuku T, Ueda A, Nagayama M (1993) *J Electrochem Soc* 140:1862
7. Delmas C, Menetrier M, Croguennec L, Saadoun I, Rougier A, Poullierie C, Prado G, Grune M, Fournes L (1999) *Electrochim Acta* 45:247
8. Ohzuku T, Komori H, Swai K, Hirai T (1990) *Chem Express* 5:733
9. Rougier A, Gravereau P, Delmas C (1996) *J Electrochem Soc* 143:1168
10. Li W, Currie JC (1997) *J Electrochem Soc* 144:2773
11. Lu CH, Lee WC (2000) *J Mater Chem* 10:1403
12. Manthiram A, Kim J (1998) *Chem Mater* 10:2903
13. Fey GTK, Shiu RF, Subranmanian V, Chen JG, Chen CL (2002) *J Power Sources* 103:265
14. Cho J, Park B (2001) *J Power Sources* 92:35
15. Ying JR, Wan CR, Jiang CY, Li YX (2001) *J Power Sources* 99:78
16. Julien C, Farh LEL, Rangan S, Massot M (1999) *J Sol Gel Sci Technol* 15:63
17. Julien C, Michael SS, Ziolkiewicz S (1999) *Int J Inorg Mater* 1:29
18. Kweona HJ, Kim GB, Lim HS, Nam SS, Park DG (1999) *J Power Sources* 83: 84
19. Alcantara R, Lavela P, Tirado JL, Zhecheva E, Stoyanova R (1998) *J Electrochem Soc* 145:730
20. Gover RKB, Kanno R, Mitchell BJ, Maseo Y, Yoji K (2000) *J Electrochem Soc* 147:4045
21. Larson AC, Dreele RBV (2000) General structure analysis system. Los Alamos National Laboratory, Los Alamos, N.M., USA
22. Song MY, Lee R (2002) *J Power Sources* 111:99
23. Hennings S, Mary W (1978) *J Solid State Chem* 26:333
24. Chang CC, Kim JY, Kumta PN (2002) *J Electrochem Soc* 149:A331
25. Morales J, Vicente CP, Tirado JL (1990) *Mater Res Bull* 25:623
26. Ohuzuku T, Ueda A, Nagayama M (1993) *J Electrochem Soc* 140:1862
27. Takahashi Y, Akimoto J, Gotoh Y, Kawaguchi K, Mizuta S (2001) *J Solid State Chem* 160:180
28. McCusker LB, Dreele RBV, Cox DE, D Louer D, Scardi P (1999) *J Appl Crystallogr* 32:36